European Journal of Nuclear Medicine and Molecular Imaging (2023) 50:4036–4050
https://doi.org/10.1007/s00259-023-06297-y

ORIGINAL ARTICLE

Comparing the clinical value of baseline [^{68} Ga]Ga-FAPI-04 PET/CT and [^{18}F]F-FDG PET/CT in pancreatic ductal adenocarcinoma: additional prognostic value of the distal pancreatitis

Jie Ding[1] · Jiangdong Qiu[2] · Zhixin Hao[1] · Hua Huang[2] · Qiaofei Liu[2] · Wenjing Liu[2] · Chao Ren[1] · Marcus Hacker[3] · Taiping Zhang[2] · Wenming Wu[2] · Xiang Li[3] · Li Huo[1]

Received: 6 April 2023 / Accepted: 5 June 2023 / Published online: 26 July 2023

Abstract

Purpose Anatomical and molecular staging strategies are needed for the personalized treatment of localized pancreatic ductal adenocarcinoma (PDAC). This study evaluated the performance of [^{68} Ga]Ga–FAPI-04 and [^{18}F]F-FDG PET/CT on the disease staging and prognostic value of patients with localized PDAC on contrast-enhanced (CE)-CT images.

Methods Patients with suspected localized PDAC on CE-CT were recruited for static [^{68} Ga]Ga-FAPI-04 and ^{18}[F]F-FDG and PET/CT, and select patients underwent simultaneous 60-min dynamic ^{68} Ga-FAPI-04 PET/CT. The diagnostic and staging performances of the static PET/CT results were evaluated by delineating regions of interest in the primary tumor, whole pancreas, and distal pancreas in both types of scans and then evaluating correlations between the PET/CT findings and clinicopathological characteristics. Furthermore, Kaplan–Meier and hazard ratio (log-rank) methods were used to evaluate the prognostic value of the combined dynamic [^{68} Ga]Ga-FAPI-04 and static [^{18}F]F-FDG PET/CT method.

Results We included 49 patients with histologically confirmed PDAC adenocarcinomas; 32 underwent 60-min dynamic [^{68} Ga]Ga-FAPI-04 PET/CT imaging simultaneously. The static [^{68} Ga]Ga-FAPI-04 method had significantly higher accuracy and uptake values than the static [^{18}F]F-FDG method for primary PDAC lesions, metastatic lymph nodes, and distal metastases. Furthermore, 18.4% and 10.2% of the patients' stages changed after using the [^{68} Ga]Ga-FAPI-04 and [^{18}F]F-FDG PET/CT methodologies, respectively, compared to the CE-CT-designated stage. The Ki values obtained from dynamic [^{68} Ga]Ga-FAPI-04 PET/CT did not differ between PDAC and distal obstructive pancreatitis lesions. Pathologically enlarged tumor size, poor differentiation, and perineural invasion were associated with increased [^{68} Ga]Ga-FAPI-04 uptake but not with [^{18}F]F-FDG uptake. The preoperative prognostic performance of [^{68} Ga]Ga-FAPI-04 was better than that of [^{18}F]F-FDG. Interestingly, combined [^{68} Ga]Ga-FAPI-04 and [^{18}F]F-FDG uptake results in the whole pancreas could further stratify patients based on their postoperative prognosis.

Conclusion ^{6}[^{68} Ga]Ga-FAPI-04 PET/CT was more sensitive and accurate than [^{18}F]F-FDG PET/CT for tumor, node, and metastasis staging of PDAC identified on CE-CT. Additionally, [^{68} Ga]Ga-FAPI-04 uptake was significantly associated with pathologically aggressive tumor features. Combined [^{68} Ga]Ga-FAPI-04 and [^{18}F]F-FDG PET/CT findings improved the prognostic value, potentially providing a non-invasive guide for clinical management. Finally, increased fibroblast activity in PDAC-induced obstructive pancreatitis may be associated with poor patient survival rates.

Keywords Pancreatic ductal adenocarcinoma · [^{18}F]F-FDG · [^{68} Ga]Ga-FAPI-04 · Tumor staging · Patient prognosis

Jie Ding and Jiangdong Qiu contributed equally to this work.

✉ Taiping Zhang
tpingzhang@yahoo.com

✉ Wenming Wu
doctorwuu@126.com

✉ Xiang Li
xiang.li@meduniwien.ac.at

✉ Li Huo
huoli@pumch.cn

Extended author information available on the last page of the article

Introduction

Pancreatic ductal adenocarcinoma (PDAC) is the most prevalent pancreatic exocrine cancer subtype [1]. Additionally, these tumors are aggressive, have a poor prognosis, and are prone to hidden extrapancreatic metastases [1, 2]. Therefore, precise initial staging and identifying distant metastases are critical for proper management.

Appropriate imaging approaches are crucial for accurately staging PDAC. Contrast-enhanced computed tomography (CE-CT) is the most recommended imaging modality for evaluating the initial stages of PDAC [1]. However, peripancreatic lymph nodes (LNs) and distant metastasis assessments are constrained by CE-CT, resulting in erroneous staging results in approximately 20% of patients [3]. The current recommendations do not advocate positron emission tomography (PET)/CT as a routine imaging modality for PDAC. However, [^{18}F]F-fluorodeoxyglucose (FDG) PET has improved staging accuracy and, thus, is often advised when distant metastases are suspected. Nevertheless, ^{18}[F] F-FDG PET/CT may occasionally lead to false-positive or false-negative interpretations of PDAC lesions [4].

PDAC is distinguished by prominent and voluminous desmoplastic stroma, with cancer-associated fibroblasts comprising more than 90% of the tumor volume [5]. Fibroblast activation protein (FAP), a membrane serine protease, is expressed in cancer-associated fibroblasts and pericytes and is a potential marker of activated stroma [6–9]. Recent studies have shown that [^{68} Ga]Ga-labeled FAP-inhibitor (FAPI) PET/CT is superior to [^{18}F]F-FDG for PDAC staging [8–10]. For example, Deng et al. suggested that [^{68} Ga] Ga-FAPI PET/CT may outperform [^{18}F]F-FDG PET/CT for identifying bone micrometastases and hidden liver metastases [11]. However, the specificity and accuracy of these two modalities for metastasis detection in patients with potentially resectable PDAC have not been well elucidated.

Notably, a prominent manifestation of [^{68} Ga]Ga-FAPI PET/CT in PDAC, particularly in the pancreatic head, is significantly elevated [^{68} Ga]Ga-FAPI uptake in the distal pancreas due to an obstructive inflammatory response, which sometimes affects the ability to identify the extent of the tumor lesion [9]. For example, patients with PDAC and jaundice have a significantly worse prognosis than no jaundice groups [12]. Interestingly, our prior study showed that preoperative [^{68} Ga]Ga-FAPI-04 parameters measured in the tumor or total pancreas were significant prognostic

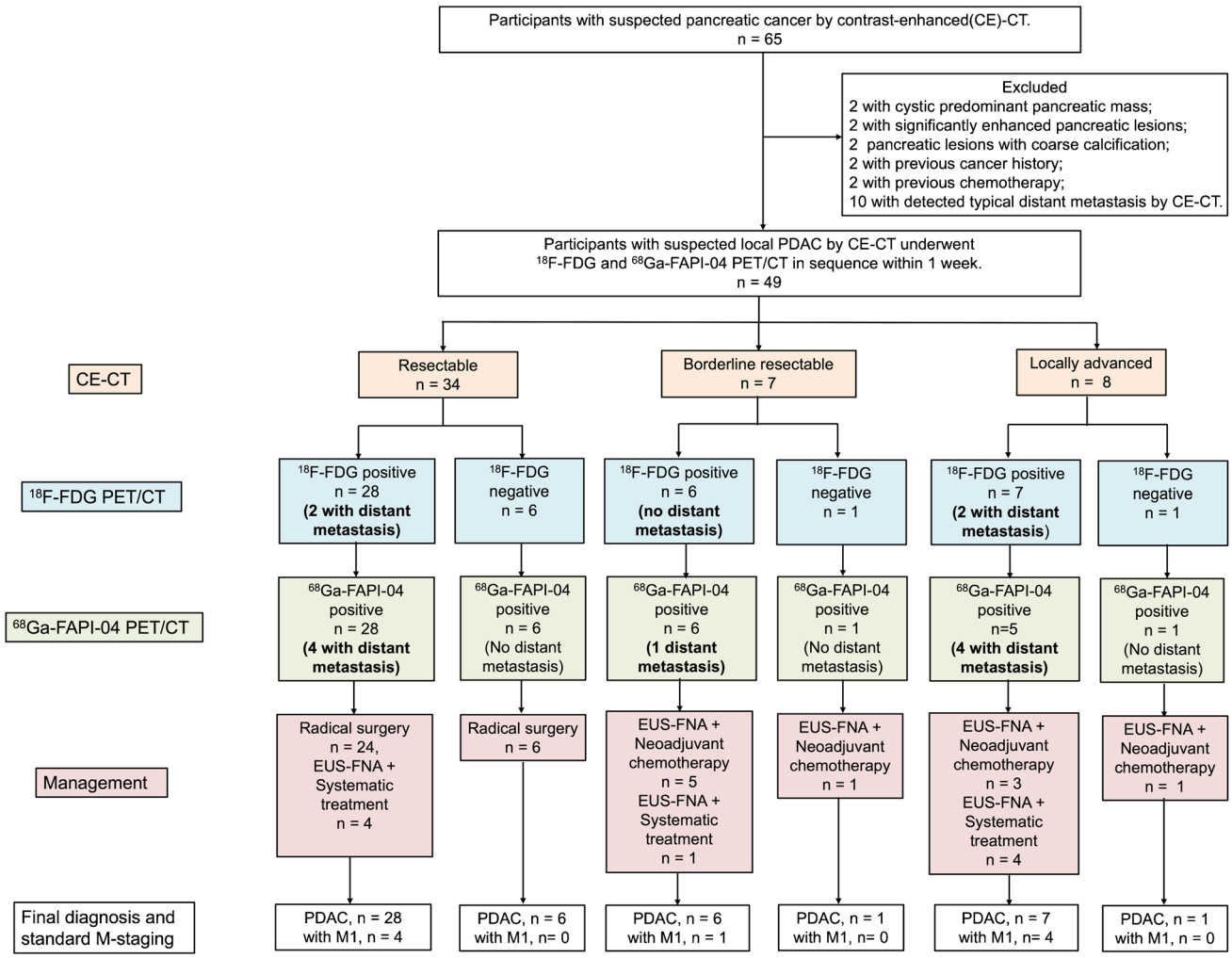

Fig. 1 The flowchart for patient imaging analysis and management. EUS-FNA, endoscopic ultrasound-guided fine-needle aspiration

predictors in patients with PDAC after surgery [13]. Therefore, the clinical significance of [^{68} Ga]Ga-FAPI-04 and [^{18}F]F-FDG and uptake in tumor-distal pancreatic tissues warrants further investigation.

This study evaluated and compared the accuracy of [^{68} Ga]Ga-FAPI-04 and [^{18}F]F-FDG PET/CT in disease staging and the impact on clinical management in patients with potentially resectable PDAC without detectable distal metastasis on CE-CT. We also evaluated the association between preoperative [^{68} Ga]Ga-FAPI-04 and [^{18}F]F-FDG PET/CT uptake and the pathological characteristics of PDAC lesions, correlations between FAPI and FDG uptake in pancreatic tissue distal to PDAC lesions and inflammation-related blood biochemical levels, and the prognostic relevance of PET/CT in PDAC lesions and pancreatic tissue postoperatively.

Materials and methods

Patients

The Institutional Ethics Committee of the Peking Union Medical College Hospital (Beijing, China, IRB protocol #ZS1810) approved this single-center prospective study, and it was registered at ClinicalTrials.gov (NCT05275985). Before taking part in this study, every participant provided written informed consent. The inclusion criteria included (1) patients with typical imaging features of PDAC in CE-CT (hypovascular pancreatic mass with irregular margins, obstructing adjacent pancreatic or bile duct) and (2) patients who underwent standard staging of PDAC without obvious detectable distant metastases by conventional imaging. Patients were excluded if they (1) had whole cystic or hypervascular pancreatic tumors; (2) had previous cancer history and anti-tumor treatment; and (3) had severe hepatic and renal insufficiency.

Of the initial sixty-five patients, forty-nine treatment-naïve patients (26 males and 23 females) with suspicion of primary PDAC finally met the inclusion criteria and were consecutively recruited between October 2020 and October 2021 finally (Fig. 1). All the enrolled patients underwent the routine preoperative staging procedures, including medical history assessment (weight loss is deemed to be present if there has been a 2 kg or greater decrease in weight during the past three months), physical examination, laboratory tests, and routine whole-body CT examination (40 patients underwent chest-abdominal-pelvic CE-CT while 9 patients underwent abdominopelvic CE-CT and separately chest plain CT). For simplicity of description, routine whole-body CT examinations are substituted with "CE-CT" when compared with PET/CT in the result part. Patients' blood biochemical parameters were recorded, including serum carbohydrate antigen 199 (CA-199), CA125, amylase, lipase, total bilirubin (TBR), alkaline phosphatase (ALP), and C-reactive protein (CPR). Our group published another research using ^{68} Ga-FAPI-04 PET/CT data from 19 patients in this article [13].

CE-CT imaging analysis

All included patients had undergone CE-CT examinations with a pancreas protocol of PUMCH. The protocol of CE-CT imaging is listed in the supplemental materials. All primary pancreatic lesions were evaluated on the tumor size (determined by its longest axis) and local resectability on CE-CT by two experienced radiologists (> 5-year experience) according to National Comprehensive

Table 1 The characteristic of the included patients

Characteristic	All participants ($n = 49$)
Number of patients	49
Male (%)	26 (53.1%)
Female (%)	23 (46.9%)
Age (years)	60.9 ± 8.9
Weight loss (%)	27 (55.1%)
Blood chemistry	
CA19-9 (U/mL)	177.0 (43.9–529.0)
CA242 (U/mL)	45.8 (9.6–111.6)
CA724 (U/mL)	3.4 (1.5–8.3)
CA125 (U/mL)	15.9 (9.8–29.1)
Amylase (U/L)	88.3 ± 57.2
Lipase (U/L)	122.0 (40.0–264.5)
TBR (μmol/L)	12.7 (8.7–62.7)
ALP (U/L)	108.0 (70.0–295.0)
NLR	3.0 ± 1.9
PLR	156.5 ± 74.4
CPR (mg/L)	1.2 (0.6–7.6)
Tumor size (cm)	4.0 ± 2.3
Tumor location	
Head/neck (%)	29 (61.2%)
Body/tail (%)	20 (38.8%)
Standard stage	
I	10 (20.4%)
II	11 (22.4%)
III	19 (38.8%)
IV	9 (18.4%)
Surgery	
Pancreatoduodenectomy (%)	18 (36.7%)
Distal pancreatectomy (%)	12 (24.5%)
EUS-FNA (%)	19 (38.8%)

TBR total bilirubin, *ALP* alkaline phosphatase, *NLR* absolute neutrophil count divided by absolute lymphocyte count, *PLR* absolute platelet count divided by absolute lymphocyte count, *CPR* C-reactive protein

Cancer Network criteria [14] (Supplementary Table 1). The resectability was classified as resectable, borderline resectable, or local advanced. Besides, regional LN with a short diameter ≥ 0.8 cm was considered positive.

PET/CT imaging analysis

The Supplemental Materials describes the synthesis of radiopharmaceuticals, the [^{68} Ga]Ga-FAPI-04 and [^{18}F]F-FDG PET/CT protocols, and the methods for image reconstruction. All patients underwent whole-body static [^{68} Ga]Ga-FAPI-04 and [^{18}F]F-FDG PET/CT 60 min after a tracer injection. Additionally, patients in good physical underwent 60-min dynamic imaging immediately after the intravenous injection of a [^{68} Ga]Ga-FAPI-04 bolus in one bed centered on the pancreas. In PET/CT scans, we employed a semi-automated spatial derivative gradient-based method (PET Edge) in by MIM Maestro v6.6 (MIM Software Inc, Cleveland, OH) for delineating regions of interest (ROI). The basis for image interpretation was identifying areas with elevated [^{18}F]F-FDG/[^{68} Ga]Ga-FAPI-04 uptake on the PET scans. If the PDAC lesions were difficult to distinguish from distal obstructive pancreatitis (especially on the [^{68} Ga]Ga-FAPI-04 PET scans), the tumor extent on the corresponding low-dose CT and CE-CT was used as an anatomical reference for delineation.

For each primary PDAC lesion, the maximum standardized uptake value (SUV_{max}), tumor metabolic volume (MTV), and total lesion glycolysis (TLG) were determined on [^{18}F]F-FDG PET/CT images, and the SUV_{max}, FAP-positive tumor volume (FTV; the lesion volume of the ROI with an SUV threshold of 40%), and the total lesion FAP expression (TLF; FTV multiplied by the corresponding mean SUV) were determined on [^{68} Ga]Ga-FAPI-04 PET/CT images.

Furthermore, The ROI of the distal pancreas is the pancreatic tissue distal to PDAC lesions and was outlined mainly with reference to CT. The ROI of the total pancreas includes PDAC lesions as well as distal pancreatic tissues, and normal pancreatic tissues proximal to PDAC are not included. Then the total pancreatic SUV_{max} ($TSUV_{max}$), distal SUV_{max} ($DSUV_{max}$), total/distal pancreatic metabolic volume (TMV/DMV), and total/distal pancreatic glycolysis (TPG/DPG) were determined on [^{18}F]F-FDG PET/CT images. The $TSUV_{max}$, $DSUV_{max}$, total/distal FAPI-avid pancreatic volume (TFV/DFV), and total/distal pancreatic FAP expression (TPF/DPF) were determined on [^{68} Ga]Ga-FAPI-04 PET/CT images. Supplemental Fig. 1 provides examples of the primary tumor and total and distal pancreatic ROI outlines.

Tumor, node, metastasis (TNM) stage based on PET/CT

The TNM stage was assessed based on the [^{68} Ga]Ga-FAPI-04 and [^{18}F]F-FDG PET/CT findings following the eighth edition of the American Joint Committee on Cancer Staging. The T-stage was based on the relationship of the pancreatic tumors to nearby vascular structures detected on CE-CT; we recorded the location, size (determined by its longest axis), and SUV_{max} of the primary pancreatic lesions. The N-stage was based on positive LNs, classified as positive if the [^{68} Ga]Ga-FAPI-04 or [^{18}F]F-FDG uptake in the LN was greater than that of the surrounding tissue. We recorded the numbers, size (determined by the shortest axis), and SUV_{max} of the positive LNs for each PET/CT scan. The M-stage was based on aberrant tracer uptake; CT images were used to evaluate distant metastases. We recorded the locations, numbers, and SUV_{max} of the distal metastases. TNM staging was performed before and after [^{68} Ga]Ga-FAPI-04 and [^{18}F]F-FDG PET/CT. We also assessed the [^{68} Ga]Ga-FAPI-04 and [^{18}F]F-FDG PET/CT findings beyond routine whole-body CT examinations (Supplementary Table 2).

The Supplemental Materials present the standard TNM staging assessments of PDAC. The TNM stages determined

Table 2 The comparison of [^{68} Ga]Ga-FAPI-04 and [^{18}F]F-FDG PET/CT in detecting lesions

	Total Number	[^{68} Ga]Ga-FAPI-04 positive number	[^{18}F]F-FDG positive number	P value	[^{68} Ga]Ga-FAPI-04 SUV_{max}	[^{18}F]F-FDG SUV_{max}	*P* value
Primary lesions	49	49 (100%)	41 (83.7%)	< 0.01	15.4 ± 8.4	6.7 ± 4.1	< 0.01
Total metastatic regional LNs	115	71 (61.7%)	42 (36.5%)	< 0.01	4.6 ± 1.8	3.7 ± 0.9	< 0.001
Metastatic regional LNs (≥ 0.8 cm)	43	41 (95.3%)	35 (81.4%)	0.09	5.4 ± 1.9	3.8 ± 0.9	< 0.001
Metastatic regional LNs (< 0.8 cm)	72	30 (41.7%)	7 (9.7%)	< 0.01	3.6 ± 0.8	3.0 ± 0.8	0.12
Metastatic regional LNs (by histopathology)	76	37 (48.7%)	19 (25.0%)	< 0.05	4.7 ± 1.8	4.1 ± 1.5	0.22
Metastatic regional LNs (by follow-up imaging)	39	34 (87.2%)	23 (60.0%)	< 0.05	4.5 ± 1.8	3.6 ± 0.8	< 0.05
Distant metastatic lesions	46	46 (100%)	22 (47.8%)	< 0.01	5.0 ± 2.2	3.1 ± 1.2	< 0.05

by the two PET/CT modalities were compared with the standard TNM classification. In addition, the sizes of the PDAC lesions measured on both PET/CT image types were compared to the standard size. A difference ± 0.5 cm was considered consistent, and a difference greater than ± 0.5 cm was considered a discrepancy.

Patient management

The management of the patients was discussed and decided by the multidisciplinary team mentioned above. Tumor radical resection was performed for patients with resectable disease. Neoadjuvant chemotherapy or chemoradiation was recommended for patients with borderline resectable and local advanced disease. Systemic chemotherapy was the primary treatment modality for patients with distant metastases. Before the chemotherapy, all patients underwent endoscopic ultrasound-guided fine-needle aspiration (EUS-FNA) to obtain a pathology diagnosis. Patients' management was recorded before and after two kinds of PET/CT (Supplementary Table 2).

Histology and survival analysis for surgery patients

All macro- and microscopic analyses of all surgical specimens were carried out by a board-certified and experienced

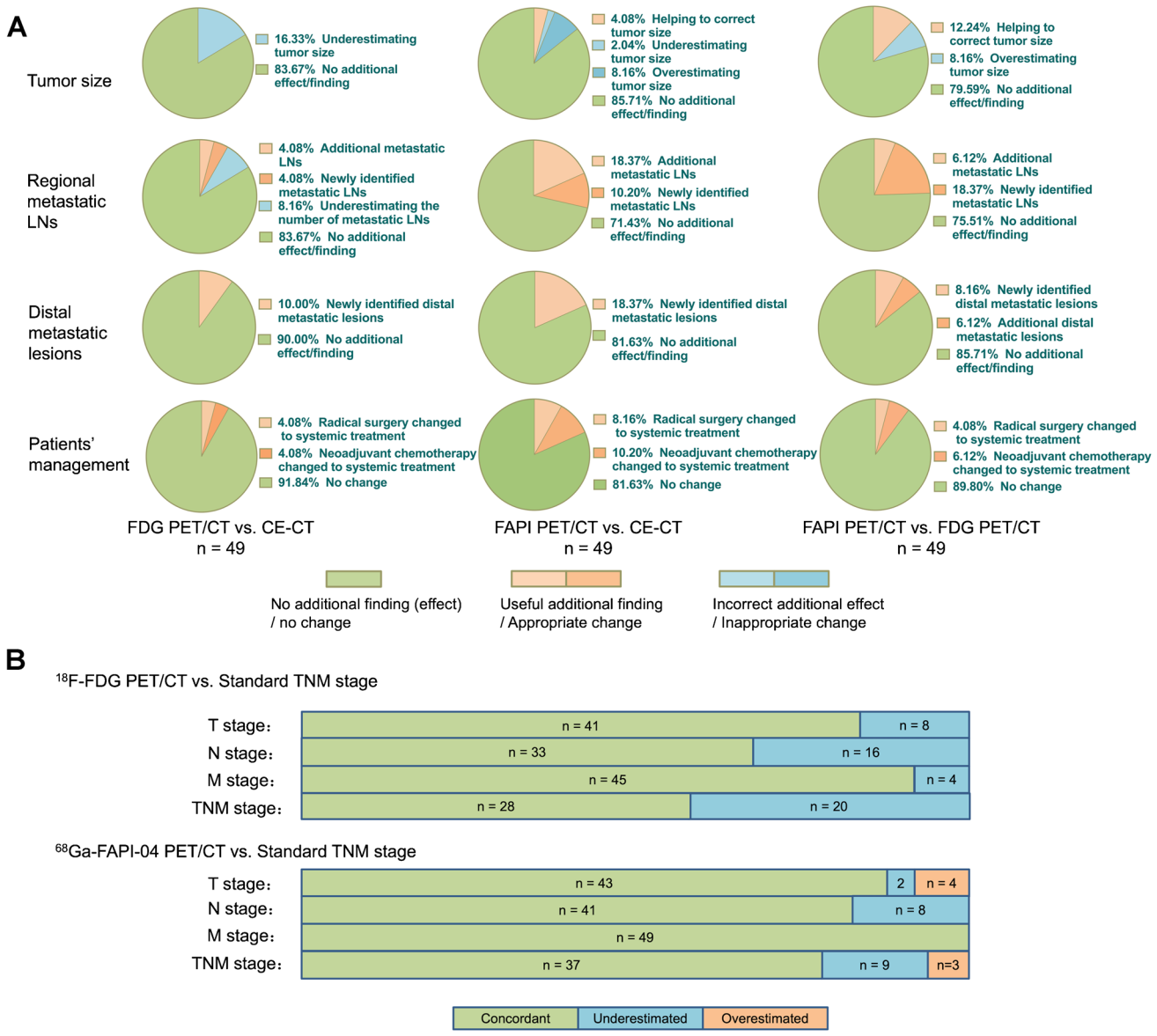

Fig. 2 **A** The additional finding and effect of patient management by [^{18}F]F-FDG PET/CT and [^{68} Ga]Ga-FAPI-04 PET/CT. **B** Alterations in TNM status ([^{18}F]F-FDG PET/CT and [.^{68} Ga]Ga-FAPI-04 PET/CT vs. standard TNM staging) in PDAC patients ($n = 49$)

oncologist (H.Z.) blinded to patients' clinical status. According to the WHO categorization system [15], the degree of difference in PDAC was classified into well, moderately, or poorly differentiated. For each PDAC specimen, the following details were recorded: tumor size (long axis diameter), grade of differentiation, perineural invasion (present or absent), N metastasis (absent or present, and the number if present) were recorded for each PDAC specimen.

For those who underwent surgery, routine (once every three to six months) laboratory and chest-abdominal-pelvis CE-CT and plain CT examinations were performed postoperatively. Recurrence-free survival (RFS) was calculated from the preoperative [^{68} Ga]Ga-FAPI-04 and [^{18}F]F-FDG PET/CT exams until the first observed cancer recurrence. Overall survival (OS) was calculated from preoperative PET/CT imaging until death. Patients without incidents were censored at the most recent clinical assessment in November 2022.

Finally, for Kaplan–Meier analyses, the surgical patients were divided into groups based on the median values of the following: (1) [^{68} Ga]Ga-FAPI-04 SUV_{max} and [^{18}F]F-FDG

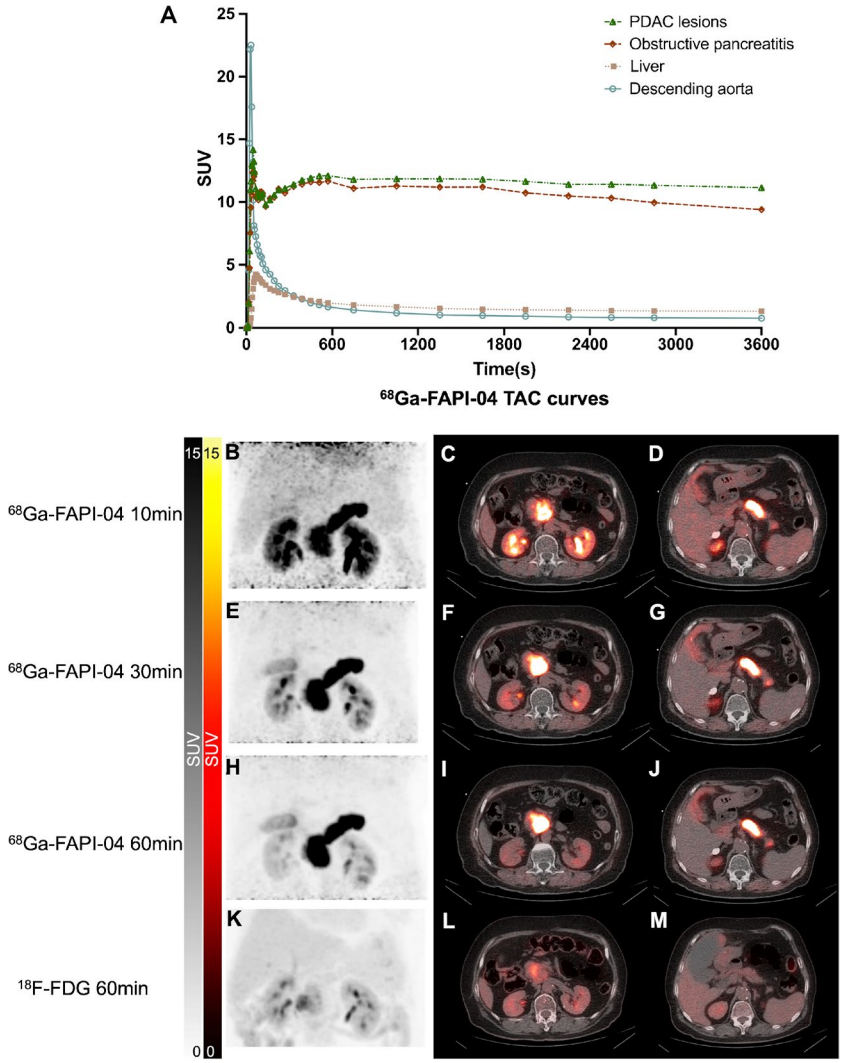

Fig. 3 (**A**) The TAC curve of PDAC and obstructive pancreatitis lesions in 1-h dynamic [^{68} Ga]Ga-FAPI-04 PET/CT. (B–M) A 72-year-old female with PDAC lesions in the pancreatic head underwent 1-h dynamic [^{68} Ga]Ga-FAPI-04 PET/CT and static [^{18}F]F-FDG PET/CT. (**B**–**D**) The images of maximum intensity projection (MIP) and axial fusion from the [^{68} Ga]Ga-FAPI-04 were reconstructed at 10 min. The MIP image showed intense uptake in the PDAC lesions companies with increased uptake of the distal obstructive pancreatitis. The SUV_{max} of PDAC and pancreatitis were 24.2 and 29.0, respectively. (**E**–**G**) Representative the images of [^{68} Ga]Ga-FAPI-04 MIP and axial fusion at 30 min. The obstructive pancreatitis lesions were still indistinguishable from PDAC lesions on PET. The SUV_{max} of PDAC and pancreatitis were 24.5 and 27.4, respectively. (H–J) The [^{68} Ga]Ga-FAPI-04 MIP and axial fusion at 60 min showed intense uptake of PDAC and distal obstructive pancreatitis. The SUV_{max} of PDAC and pancreatitis were 25.2 and 23.1, respectively. K-M. The pancreas-centered MIP image of static [^{18}F]F-FDG PET/CT at 60 min. The PDAC lesions showed unevenly elevated uptake ($SUV_{max} = 10.8$) without increased uptake in the distal pancreas

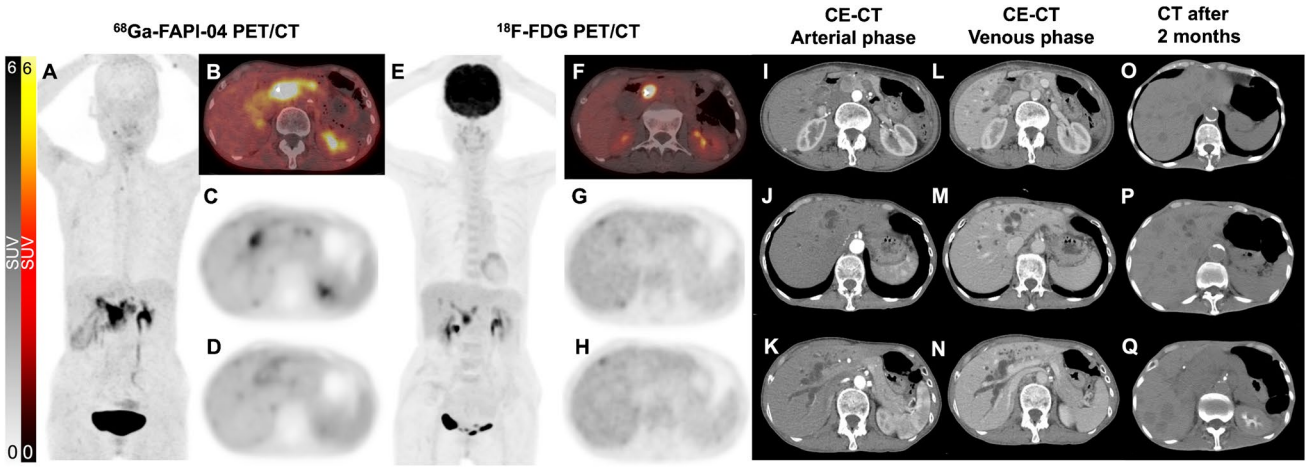

Fig. 4 A 55-year-old female patient with abdominal pain and weight loss for two months. The MIP, PET, and axial fusion from the [^{68} Ga]Ga-FAPI-04 (**A**–**D**) showed increased uptake in the PDAC lesions in the pancreas. (SUV_{max} = 12.5) and multiple liver metastases with focal [^{68} Ga]Ga-FAPI-04 uptake (SUV_{max} = 1.4–3.0). (E–H) The image of MIP, PET, and axial fusion of ^{18}[F]F-FDG showed moderate uptake in the primary pancreatic lesion (SUV_{max} = 7.2) and multiple liver metastases (SUV_{max} = 2.1–2.7). The tumor size showed in [^{68} Ga]Ga-FAPI-04 PET/CT was larger than in [^{18}F]F-FDG PET/CT. Besides, the number of liver lesions detected in [^{18}F]F-FDG PET/CT was less than [^{68} Ga]Ga-FAPI-04 PET/CT. (I–N) The axial arterial phase and venous phase of CE-CT images at the time of inclusion showed dilated bile ducts, but no liver metastases were observed. (O–Q) CT scan after two months shows multiple liver metastases

SUV_{max}; (2) [^{68} Ga]Ga-FAPI-04 FTV and [^{18}F]F-FDG MTV; (3) [^{68} Ga]Ga-FAPI-04 TLF and [^{18}F]F-FDG TLG; (4) [^{68} Ga]Ga-FAPI-04 $TSUV_{max}$ and [^{18}F]F-FDG $TSUV_{max}$; (5) [^{68} Ga]Ga-FAPI-04 TFV and [^{18}F]F-FDG TMV; and (6) [^{68} Ga]Ga-FAPI-04 TPF and [^{18}F]F-FDG TPG.

Statistical analysis

PASW (version 18.0; SPSS, Inc., Chicago, IL, USA) and GraphPad Prism 8 statistical software were used to perform the statistical analyses. The mean ± standard deviation or median and interquartile range were used to express quantitative values. The statistical methods were detailed in a list in the supplemental materials. Statistical significance was set at $P < 0.05$.

Results

Clinical characteristics of patients

We recruited 49 patients; Table 1 presents their clinical characteristics. All patients had a final histological PDAC diagnosis, 30 underwent radical surgery, and 19 underwent endoscopic ultrasound-guided fine-needle aspiration. The

Table 3 The correlation between imaging and pathological features in PDAC lesions (n = 30)

PET/CT parameters	S	D	St	P	L	Ln
FDG SUV_{max}	**0.54****	0.33	0.02	0.27	0.25	0.18
FDG MTV	0.33	0.09	−0.09	0.15	0.14	0.08
FDG TLG	**0.51***	0.28	0.03	0.28	0.24	0.17
FAPI SUV_{max}	**0.37***	**0.69****	0.10	**0.59****	0.12	0.18
FAPI FTV	**0.37***	**0.43***	0.05	0.22	0.17	0.10
FAPI TLF	**0.53****	**0.74****	0.06	**0.46****	0.20	0.19
FDG TMV	0.08	0.11	0.17	0.21	**0.49****	0.29
FDG TPG	**0.49****	−0.03	−0.05	−0.12	0.25	0.04
FAPI $TSUV_{max}$	**0.46***	**0.72****	−0.03	**0.54****	0.12	0.11
FAPI TFV	0.17	0.16	0.26	0.16	**0.49****	0.25
FAPI TPF	0.22	**0.39***	0.09	0.34	0.35	0.15

Bold values indicate that the corresponding correlation coefficients are statistically significant

S tumor size, *D* tumor differentiation, *St* pathological TNM stage, *P* perineural invasion, *L* lymph nodes metastases, *Ln* the number of metastatic lymph nodes

*$P < 0.05$; **$P < 0.01$

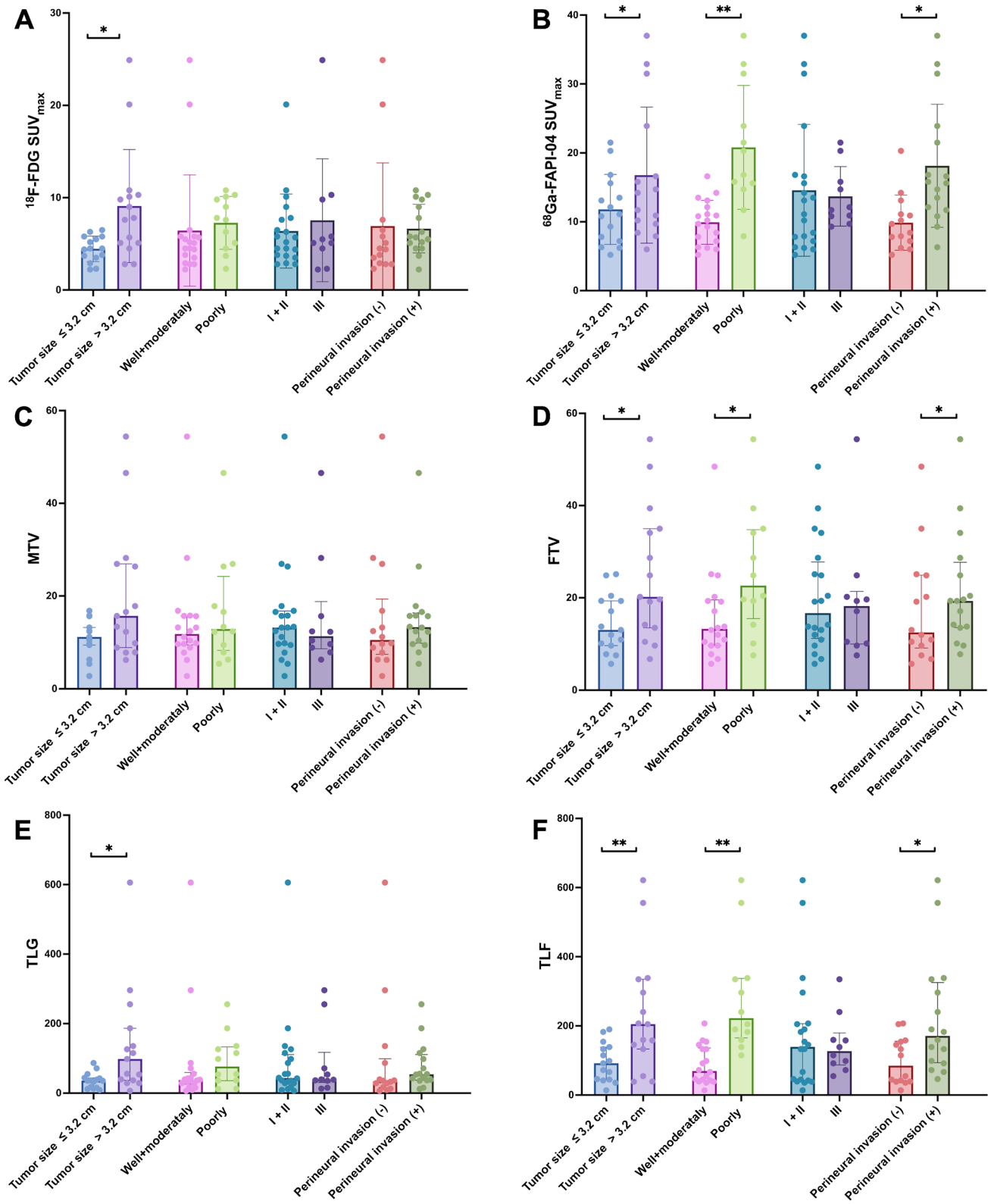

Fig. 5 The difference in [^{18}F]F-FDG and [^{68} Ga]Ga-FAPI-04 PET/CT parameters between different histopathology groups: **A** [^{18}F]F-FDG SUV_{max}, **B** [^{68}Ga]Ga-FAPI-04 SUV_{max}, **C** [^{18}F]F-FDG MTV, **D** [^{68}Ga]Ga-FAPI-04 FTV, **E** [^{18}F]F-FDG TLG and **F** [^{68}Ga]Ga-FAPI-04 TLF

time interval between imaging and surgery or biopsy did not exceed 20 days. During the follow-up period (median: 17 [range, 11–26] months), 24 of 30 patients who underwent surgery experienced recurrences, and 12 died. Of the 19 patients who did not undergo radical surgery, 10 received neoadjuvant chemotherapy (borderline resected/locally advanced without distal metastases), and nine were treated with systemic chemotherapy because of distal metastases.

Primary PDAC lesion assessment: T-staging

Overall, 34 of 49 patients had resectable lesions. Based on CE-CT, seven patients had borderline resectable lesions, and eight had locally advanced PDAC lesions (Fig. 1). The [^{68} Ga]Ga-FAPI-04 positivity rate for PDAC lesions was significantly higher than that of [^{18}F]F-FDG (100% vs. 83.7%, $P<0.01$). Eight patients showed no increased uptake on [^{18}F]F-FDG PET/CT (Supplemental Fig. 2), mainly in the resectable group ($n=6$). In the primary PDAC lesions, the mean [^{68} Ga]Ga-FAPI-04 SUV_{max} was significantly higher than that of [^{18}F]F-FDG PET/CT (Table 2). However, the [^{68} Ga]Ga-FAPI-04 SUV_{max} did not differ between the FDG-positive and FDG-negative groups ($SUV_{max}=16.1\pm8.7$ vs. 13.1 ± 4.8, $P=0.34$).

Since PET/CT was performed as a low-dose CT scan without intravenous contrast, vascular invasion of the primary pancreatic lesions was primarily assessed using CE-CT. In this investigation, bias in the primary lesion's size was the key factor influencing PET/CT for T-stage evaluations in patients with PDAC. The size was incorrectly underestimated in [^{18}F]F-FDG PET/CT relative to the CE-CT findings in eight patients. Five patients had erroneous size evaluations (one underestimation and four overestimations) after [^{68} Ga]Ga-FAPI-04 PET/CT. Therefore, the [^{68} Ga]Ga-FAPI-04 PET/CT was more accurate than the [^{18}F]F-FDG PET/CT for assessing the T-stage (Fig. 2).

Kinetic modeling of ^{68} Ga-FAPI-04 between PDAC and obstructive pancreatitis

In total, 28 patients had PDAC-induced distal obstructive pancreatitis with increased radioactivity uptake on [^{68} Ga]

Table 4 The univariate analysis of predictive factors for RFS and OS for surgery patients ($n=30$)

Variables	RFS			OS		
	HR	95% CI	*P* value	HR	95% CI	*P* value
Size > 3.2 cm	**2.39**	**0.96–5.94**	**< 0.05**	1.73	0.47–6.42	0.40
CA125 > 13.8 U/mL	**2.67**	**0.93–7.64**	**< 0.05**	**3.98**	**0.72–21.94**	**< 0.05**
CA199 > 153.0 U/mL	1.26	0.54–2.97	0.82	1.47	0.39–5.51	0.55
Amylase	0.87	0.39–1.95	0.71	0.39	0.11–1.36	0.15
Lipase	1.44	0.65–3.21	0.34	1.04	0.30–3.60	0.95
TBR	**2.15**	**0.95–4.88**	**< 0.05**	2.69	0.74–9.79	0.09
ALP	1.73	0.77–3.92	0.15	1.51	0.43–5.36	0.48
CPR	**2.13**	**0.94–4.82**	**< 0.05**	1.20	0.35–4.18	0.76
PDAC lesions						
FDG SUV_{max} > 5.4	1.31	0.59–2.92	0.48	1.01	0.29–3.47	0.99
FDG MTV > 12.4	0.91	0.39–2.14	0.83	2.35	0.66–8.36	0.15
FDG TLG > 40.8	1.33	0.59–2.98	0.46	1.32	0.38–4.62	0.65
FAPI SUV_{max} > 11.9	**2.90**	**1.27–6.67**	**0.004**	5.24	**1.50–18.32**	**0.02**
FAPI FTV > 18.1	1.91	0.84–4.34	0.08	2.84	**0.77–10.45**	**0.07**
FAPI TLF > 136.0	1.84	0.81–4.17	0.11	**7.34**	**2.01–26.87**	**0.001**
Total pancreas						
FDG TMV > 30.9	1.45	0.64–3.27	0.33	2.61	0.72–9.47	0.10
FDG TPG > 81.9	1.57	0.69–3.57	0.22	2.57	0.71–9.30	0.10
FAPI $TSUV_{max}$ > 14.5	**3.65**	**1.50–8.92**	**0.004**	**5.24**	**1.50–18.32**	**0.02**
FAPI FPV > 45.6	1.85	0.80–4.29	0.09	**4.65**	**1.25–17.30**	**0.008**
FAPI TPF > 284.5	**3.83**	**1.53–9.61**	**0.004**	**18.39**	**5.71–59.20**	**0.0003**
Distal pancreas						
FDG $DSUV_{max}$ > 2.0	1.01	0.40–2.55	0.99	0.52	0.12–2.36	0.38
FDG DMV > 15.3	1.77	0.79–3.97	0.13	2.01	0.57–7.04	0.26
FDG DPG > 25.4	1.41	0.63–3.13	0.37	1.80	0.52–6.25	0.35
FAPI $DSUV_{max}$ > 8.0	**2.42**	**0.90–6.46**	**< 0.05**	2.57	0.58–11.29	0.23
FAPI DFV > 22.2	1.39	0.62–3.12	0.39	1.74	0.48–6.31	0.34
FAPI DPF > 55.5	1.54	0.60–3.25	0.35	1.84	0.51–6.42	0.31

The bold values indicate that the corresponding *P* value are less than 0.05

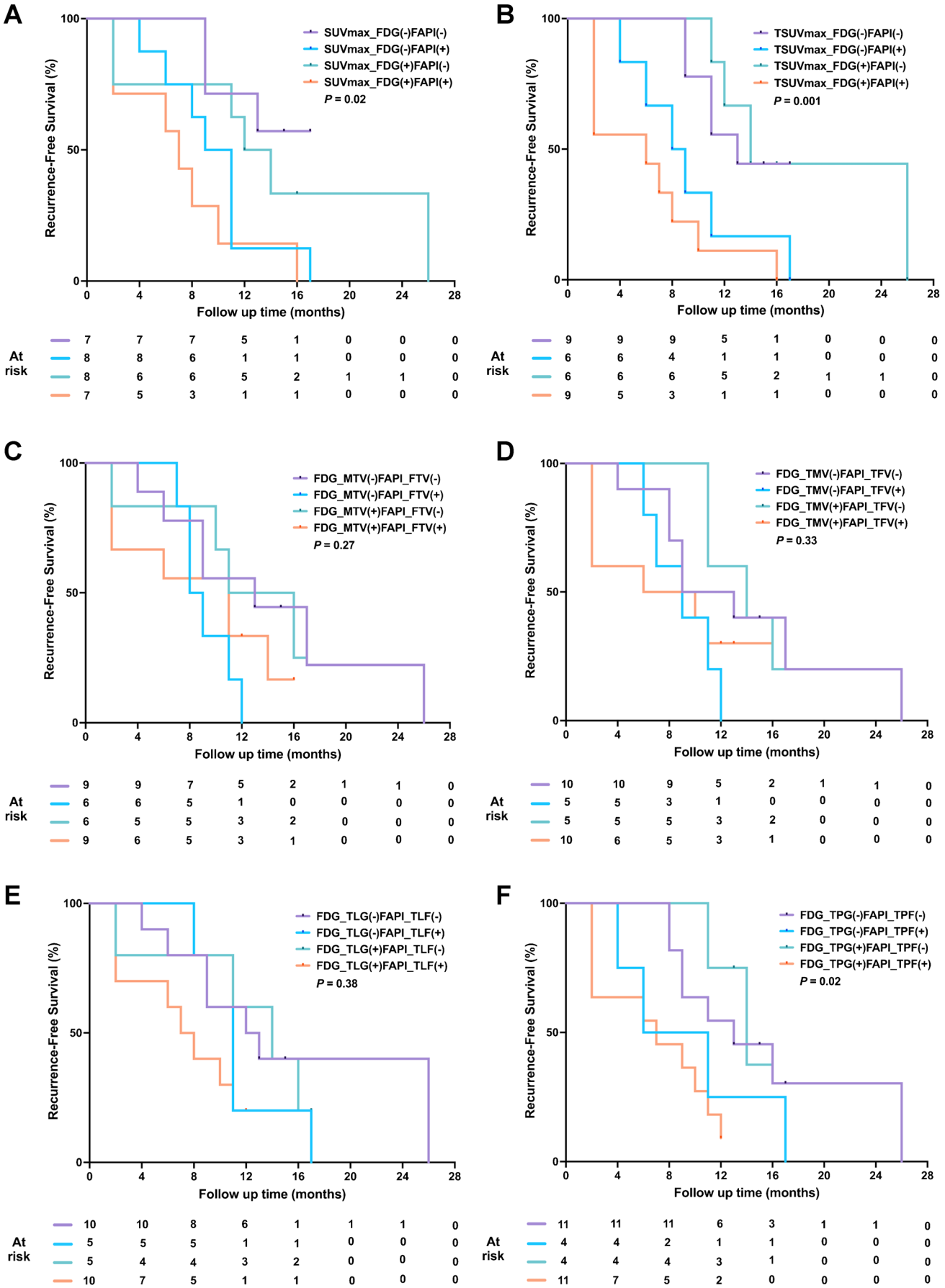
A
Recurrence-Free Survival (%)
Follow up time (months)
SUVmax_FDG(-)FAPI(-)
SUVmax_FDG(-)FAPI(+)
SUVmax_FDG(+)FAPI(-)
SUVmax_FDG(+)FAPI(+)
P = 0.02
At risk
7 7 7 5 1 0 0 0
8 8 6 1 1 0 0 0
8 6 6 5 2 1 1 0
7 5 3 1 1 0 0 0
B
TSUVmax_FDG(-)FAPI(-)
TSUVmax_FDG(-)FAPI(+)
TSUVmax_FDG(+)FAPI(-)
TSUVmax_FDG(+)FAPI(+)
P = 0.001
At risk
9 9 9 5 1 0 0 0
6 6 4 1 1 0 0 0
6 6 6 5 2 1 1 0
9 5 3 1 1 0 0 0
C
FDG_MTV(-)FAPI_FTV(-)
FDG_MTV(-)FAPI_FTV(+)
FDG_MTV(+)FAPI_FTV(-)
FDG_MTV(+)FAPI_FTV(+)
P = 0.27
At risk
9 9 7 5 2 1 1 0
6 6 5 1 0 0 0 0
6 5 5 3 2 0 0 0
9 6 5 3 1 0 0 0
D
FDG_TMV(-)FAPI_TFV(-)
FDG_TMV(-)FAPI_TFV(+)
FDG_TMV(+)FAPI_TFV(-)
FDG_TMV(+)FAPI_TFV(+)
P = 0.33
At risk
10 10 9 5 2 1 1 0
5 5 3 1 0 0 0 0
5 5 5 3 2 0 0 0
10 6 5 3 1 0 0 0
E
FDG_TLG(-)FAPI_TLF(-)
FDG_TLG(-)FAPI_TLF(+)
FDG_TLG(+)FAPI_TLF(-)
FDG_TLG(+)FAPI_TLF(+)
P = 0.38
At risk
10 10 8 6 1 1 1 0
5 5 5 1 1 0 0 0
5 4 4 3 2 0 0 0
10 7 5 1 1 0 0 0
F
FDG_TPG(-)FAPI_TPF(-)
FDG_TPG(-)FAPI_TPF(+)
FDG_TPG(+)FAPI_TPF(-)
FDG_TPG(+)FAPI_TPF(+)
P = 0.02
At risk
11 11 11 6 3 1 1 0
4 4 2 1 1 0 0 0
4 4 4 3 1 0 0 0
11 7 5 2 0 0 0 0

◂**Fig. 6** Representative Kaplan Meier plots of RFS in 30 resectable PDAC patients. The Kaplan Meier plots stratified by **A** the median of [^{18}F]F-FDG and [^{68} Ga]Ga-FAPI-04 SUV_{max}, **B** the median of [^{18}F]F-FDG $TSUV_{max}$ (=SUV_{max}) and [^{68} Ga]Ga-FAPI-04 $TSUV_{max}$, **C** the median of [^{18}F]F-FDG MTV and [^{68} Ga]Ga-FAPI-04 FTV, **D** the median of [^{18}F]F-FDG TMV and [^{68} Ga]Ga-FAPI-04 TFV, **E** the median of [^{18}F]F-FDG TLG and [^{68} Ga]Ga-FAPI-04 TLF, and **F** the median of [^{18}F]F-FDG TPG and [^{68} Ga]Ga-FAPI-04 TPF

Ga-FAPI-04 PET/CT, of which 13 obstructive pancreatitis lesions were indistinguishable from the PDAC lesions on PET images (SUV_{max} = 13.3 ± 9.5). In contrast, only five patients had obstructive pancreatitis with increased uptake on ^{18}[F]F-FDG PET/CT, and all were distinguishable from the pancreatic cancer lesions (SUV_{max} = 4.0 ± 1.0).

Moreover, 32 patients underwent a 60-min dynamic [^{68} Ga]Ga-FAPI-04 PET/CT examination, and 23 had obstructive pancreatitis with increased uptake. Figure 3 presents the time-activity curves (TAC). The SUV degree of decline was greater in the pancreatitis lesions than in the PDAC lesions, but within one hour, significant differences between the two were not observed (SUV_{max} = 11.15 ± 5.3 vs. 9.4 ± 7.2 at 1 h, P = 0.31). Furthermore, the pancreatitis lesion and PDAC dynamic Ki values did not differ (0.23 ± 0.24 vs. 0.32 ± 0.26; P = 0.19).

Metastatic regional LN diagnoses: N-staging

In total, 76 metastatic LNs were pathologically confirmed in 16 patients. In the patient-based analysis, the sensitivity and accuracy of [^{68} Ga]Ga-FAPI-04 for N-staging were 56.3% (9/16) and 76.7% (23/30), respectively; these values were better than those for [^{18}F]F-FDG (sensitivity: 31.3% [5/16]; accuracy: 63.3% [19/30]). Notably, PET/CT did not overestimate the T-stage. The LN metastasis detection rates were 48.7% (37/76) for [^{68} Ga]Ga-FAPI-04 and 25.0% (19/76) for [^{18}F]F-FDG.

Based on the follow-up radiographic examinations, 39 metastatic LNs were diagnosed in 14 of 19 patients who did not undergo surgery. The [^{68} Ga]Ga-FAPI-04 and [^{18}F]F-FDG PET/CT sensitivities were 100.0% and 71.4%, respectively. [^{68} Ga]Ga-FAPI-04 PET/CT detected significantly more metastatic LNs than [^{18}F]F-FDG PET/CT (87.2% vs. 60.0%; n = 34 vs. 23, respectively), none of which were false positives.

[^{68} Ga]Ga-FAPI-04 had a significantly higher SUV_{max} than [^{18}F]F-FDG (P < 0.001) in the metastatic LNs. Compared to CE-CT, [^{68} Ga]Ga-FAPI-04 and [^{18}F]F-FDG PET/CT showed additional findings in the regional LN assessments (Supplemental Fig. 3). All additional [^{68} Ga]Ga-FAPI-04 discoveries were beneficial, but the [^{18}F]F-FDG findings were both beneficial and detrimental (Fig. 2 and Table 2).

Distant metastatic lesion diagnoses: M-staging

Nine patients with PDAC had distant metastases, including six with liver metastasis, one with peritoneal and bone metastasis, one with peritoneal metastasis, and one with lymph node metastasis in the supraclavicular fossa. [^{68} Ga]Ga-FAPI-04 and [^{18}F]F-FDG PET/CT outperformed CE-CT for detecting metastatic lesions (Fig. 4). [^{68} Ga]Ga-FAPI-04 PET/CT correctly identified distant metastases in nine (100%) patients, but ^{18}[F]F-FDG PET/CT only identified liver metastases in five of nine (55.5%) patients. In total, 46 distant metastases were confirmed, with a detection efficiency of 100% for ^{68} Ga-FAPI-04 PET/CT compared to only 47.8% for [^{18}F]F-FDG PET/CT. The [^{68} Ga]Ga-FAPI-04 SUV_{max} for distant metastases was also higher than that of [^{18}F]F-FDG (Table 2, P < 0.05).

In summary, compared to CE-CT, [^{68} Ga]Ga-FAPI-04 PET detected more lesions in 18 of 49 patients (36.7%) and [^{18}F]F-FDG PET/CT in 17 of 49 patients (34.7%). Most noticeably, seven of these patients had metastases to regional LNs, and four had distal metastatic lesions only on [^{68} Ga]Ga-FAPI-04 PET/CT. The TNM staging of 75.5% (37/49) and 55.1% (20/36) of the patients was accurately evaluated using [^{68} Ga]Ga-FAPI-04 PET/CT and [^{18}F]F-FDG PET/CT, respectively.

Clinical management

Both [^{18}F]F-FDG and [^{68} Ga]Ga-FAPI-04 PET/CT showed additional distant metastasis findings that could be valuable for treatment selection compared to CE-CT. [^{18}F]F-FDG PET/CT helped five patients' management (Fig. 2). Additional [^{68} Ga]Ga-FAPI-04 PET/CT findings resulted in treatment changes in nine patients (18.4%) compared to the proposed treatment based on CE-CT (Fig. 2). In addition, [^{68} Ga]Ga-FAPI-04 PET/CT findings modified the treatment plan of four patients (8.1%) relative to the treatment plan based on the [^{18}F]F-FDG PET/CT findings (Fig. 3). These patients with appropriate patients' management change by [^{68} Ga]Ga-FAPI-04 PET/CT had higher serum carbohydrate antigen (CA)19–9 and CA125 levels and larger tumor sizes than patients with no treatment effects (Supplemental Table 3).

Relationships between PET/CT and biochemical features

Supplemental Table 4 illustrates the relationships between PET/CT parameters and biochemical features. The serum CA125 level had a stronger correlation with PET parameters than the serum CA199 level. Serum CPR significantly correlated with pancreatic [^{18}F]F-FDG and [^{68} Ga]Ga-FAPI-04 avid volume and uptake in PDAC lesions, as well as in the total pancreas. The blood inflammatory indicators amylase, lipase, TBR, and ALP correlated the most strongly with the PET imaging characteristics of the distal pancreas. The correlation between the imaging parameters and these blood biochemical indicators was significantly higher with [^{68} Ga]Ga-FAPI-04 PET/CT than with [^{18}F]F-FDG PET/CT.

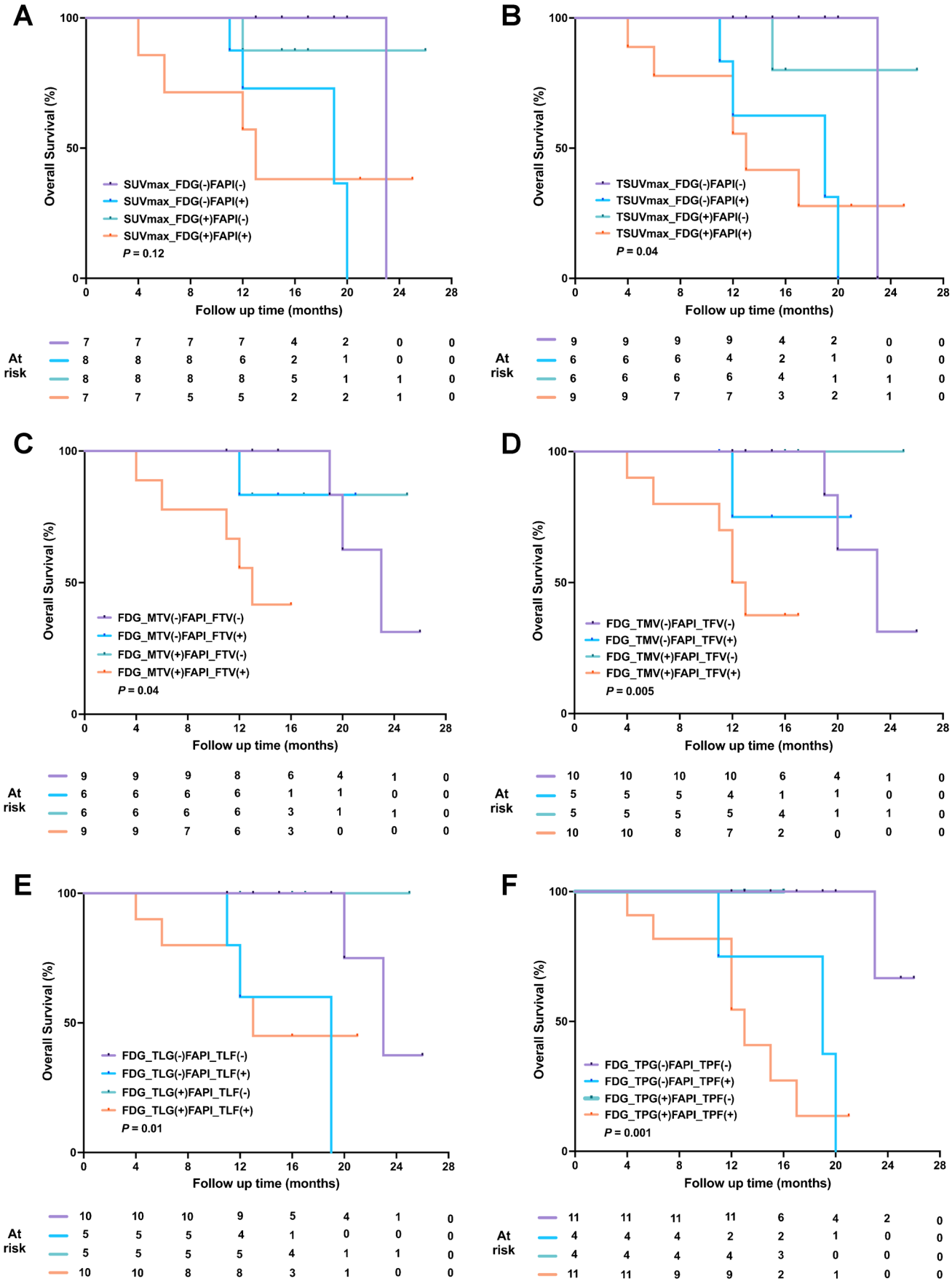
A
Overall Survival (%)
Follow up time (months)
SUVmax_FDG(-)FAPI(-)
SUVmax_FDG(-)FAPI(+)
SUVmax_FDG(+)FAPI(-)
SUVmax_FDG(+)FAPI(+)
P = 0.12
At risk
7 7 7 7 4 2 0 0
8 8 8 6 2 1 0 0
8 8 8 8 5 1 1 0
7 7 5 5 2 2 1 0
B
TSUVmax_FDG(-)FAPI(-)
TSUVmax_FDG(-)FAPI(+)
TSUVmax_FDG(+)FAPI(-)
TSUVmax_FDG(+)FAPI(+)
P = 0.04
At risk
9 9 9 9 4 2 0 0
6 6 6 4 2 1 0 0
6 6 6 6 4 1 1 0
9 9 7 7 3 2 1 0
C
FDG_MTV(-)FAPI_FTV(-)
FDG_MTV(-)FAPI_FTV(+)
FDG_MTV(+)FAPI_FTV(-)
FDG_MTV(+)FAPI_FTV(+)
P = 0.04
At risk
9 9 9 8 6 4 1 0
6 6 6 6 1 1 0 0
6 6 6 6 3 1 1 0
9 9 7 6 3 0 0 0
D
FDG_TMV(-)FAPI_TFV(-)
FDG_TMV(-)FAPI_TFV(+)
FDG_TMV(+)FAPI_TFV(-)
FDG_TMV(+)FAPI_TFV(+)
P = 0.005
At risk
10 10 10 10 6 4 1 0
5 5 5 4 1 1 0 0
5 5 5 5 4 1 1 0
10 10 8 7 2 0 0 0
E
FDG_TLG(-)FAPI_TLF(-)
FDG_TLG(-)FAPI_TLF(+)
FDG_TLG(+)FAPI_TLF(-)
FDG_TLG(+)FAPI_TLF(+)
P = 0.01
At risk
10 10 10 9 5 4 1 0
5 5 5 4 1 0 0 0
5 5 5 5 4 1 1 0
10 10 8 8 3 1 0 0
F
FDG_TPG(-)FAPI_TPF(-)
FDG_TPG(-)FAPI_TPF(+)
FDG_TPG(+)FAPI_TPF(-)
FDG_TPG(+)FAPI_TPF(+)
P = 0.001
At risk
11 11 11 11 6 4 2 0
4 4 4 2 2 1 0 0
4 4 4 4 3 0 0 0
11 11 9 9 2 1 0 0

◂**Fig.7** Representative the Kaplan Meier plots of OS in 30 resectable PDAC patients. The Kaplan Meier plots stratified by **A** the median of [^{18}F]F-FDG and [^{68} Ga]Ga-FAPI-04 SUV_{max}, **B** the median of [^{18}F]F-FDG $TSUV_{max}$ (=SUV_{max}) and [^{68} Ga]Ga-FAPI-04 $TSUV_{max}$, **C** the median of [^{18}F]F-FDG MTV and [^{68} Ga]Ga-FAPI-04 FTV, **D** the median of [^{18}F]F-FDG TMV and [^{68} Ga]Ga-FAPI-04 TFV, **E** the median of [^{18}F]F-FDG TLG and [^{68} Ga]Ga-FAPI-04 TLF, and **F** the median of [^{18}F]F-FDG TPG and [^{68} Ga]Ga-FAPI-04 TPF

Relationships between PET/CT parameters and tumor pathological features

Table 3 presents the correlations between [^{68} Ga]Ga-FAPI-04 and [^{18}F]F-FDG uptake and tumor histopathological characteristics in the 30 patients who underwent surgery, and Fig. 5 illustrates the differences in PET/CT parameters between the different pathological groups. [^{18}F]F-FDG uptake positively correlated with lesion size, and [^{68} Ga]Ga-FAPI-04 uptake strongly and positively correlated with tumor size, differentiation level, and perineural invasion.

Survival analysis for surgery patients

Table 4 presents the univariate analysis results for RFS and OS in the 30 patients who underwent radical surgery. The multivariate analysis (Supplemental Table 5) showed that [^{68} Ga]Ga-FAPI-04 $TSUV_{max}$ was a significant independent prognostic factor for RFS (hazard ratio [HR] = 4.41, $P < 0.01$), and [^{68} Ga]Ga-FAPI-04 TPF was an independent prognostic factor for OS (HR = 16.16, $P < 0.05$). Furthermore, [^{68} Ga]Ga-FAPI-04 PET/CT demonstrated superior performance for preoperative prognostication compared to [^{18}F]F-FDG PET/CT. Interestingly, the group with concurrent high tumor and pancreatic [^{18}F]F-FDG and [^{68} Ga]Ga-FAPI-04 uptake had a worse RFS and OS prognoses, especially based on the PET/CT parameters in the total pancreas (Figs. 6 and 7).

Discussion

Clinical staging is essential for predicting survival and selecting management options for patients with PDAC. Therefore, for potential surgical candidates with PDAC who have no evident distant metastases on conventional CE-CT, it is crucial to utilize whole-body PET/CT for a more accurate staging assessment. ^{18}[F]F-FDG PET/CT had a limited role in PDAC staging and surgical planning [4], which allowed for the refinement of PET descriptors to help stratify patients with PDAC and improve the method's prognostic accuracy. We found that the sensitivity and accuracy were better with the new [^{68} Ga]Ga-FAPI-04 PET/CT M-staging strategy than with the [^{18}F]F-FDG PET/CT strategy. Therefore, in vivo quantification of tumor and total pancreatic metabolism and microenvironment activation by [^{18}F]F-FDG and [^{68} Ga]Ga-FAPI-04 PET/CT could ultimately help with prognostic stratification. Overall, we found that quantitative uptake assessments on PET/CT allowed for preoperative staging and identified additional PET/CT-related prognostic factors, which were the key findings of this study.

In our study, 16.3% of primary PDAC lesions were non-FDG-avid, but the [^{68} Ga]Ga-FAPI-04 SUV_{max} did not differ between the FDG-avid and non-FDG-avid lesions. Reports suggest that in vitro and in vivo FDG absorptions are critically dependent on the cellularity of tumor cells. Therefore, awareness of the potential for false-negative results owing to low cellularity, even in large PDAC lesions, is important [16]. In addition, PDAC manifests as a hypo-[^{68} Ga]Ga-FAPI-04-uptake mass localized in the pancreatic head and neck and presents an oversized tumor volume compared to its presentation on CE-CT. In addition, we discovered that for pancreatic head/neck PDAC lesions, [^{68} Ga]Ga-FAPI-04 PET/CT tends to overestimate the size of tumors compared to CE-CT. This finding may also be related to the misleading uptake of drugs for obstructive pancreatitis, and other studies have shown that 3-h delayed scans may help differentiate malignant lesions from pancreatitis [8, 9]. Together, this suggests that PDAC and pancreatitis have different hemodynamic characteristics. However, we performed a 60-min dynamic [^{68} Ga]Ga-FAPI-04 PET/CT examination in patients with PDAC, and the radiokinetics for pancreatic cancer and pancreatitis were comparable. Thus, discriminating primary tumors from obstructive pancreatitis lesions using the SUV or kinetic parameters is impractical in most patients with PDAC. Additionally, [^{68} Ga]Ga-FAPI-04 was inferior to CE-CT for assessing the extent of PDAC lesions. Although previous research showed that FAP radionuclide-targeted therapy is feasible in animal experiments [17], our dynamic study indicates that kind of therapy may not be suitable for PDAC patients combined with distal obstructive pancreatitis.

LN metastasis is crucial for clinical management as it is an independent prognostic indicator [18]. However, identifying pathological LN metastases in PDAC was limited using preoperative CE-CT exams because malignant LNs may be smaller than 0.8 cm, and CT nodal enlargement is not very specific for indicating metastasis. In our investigation, [^{68} Ga]Ga-FAPI-04 PET/CT detected more metastatic LNs than [^{18}F]F-FDG PET/CT, redefining clinical N-staging. Moreover, the fundamental benefit of PET/CT as a whole-body imaging technique is its ability to identify distant metastases, which is a crucial factor in treatment decision-making. We found that both the sensitivity and accuracy of [^{68} Ga]Ga-FAPI-04 PET/CT were better than [^{18}F]F-FDG PET/CT for metastatic staging. PDAC patients with a higher risk of metastasis (such as higher serum CA19-9 and CA125 levels, and bigger tumor sizes) on clinical indicators might more likely to see extra findings with [^{68} Ga]Ga-FAPI-04 PET/CT in addition to CE-CT.

We found that [^{68} Ga]Ga-FAPI-04 uptake, rather than [^{18}F]F-FDG uptake, in localized PDAC is significantly correlated

with aggressive pathological characteristics. We further discovered a substantial association between [^{68} Ga]Ga-FAPI-04 uptake of the distal pancreas and blood biochemical inflammatory markers. Besides, [^{68} Ga]Ga-FAPI-04 PET/CT showed improved performance for preoperative prognostication in comparison to [^{18}F]F-FDG. Since previous article showed that obstructive pancreatitis is associated with shorter OS in patients with PDAC [12]. We delineated the ROI of the whole pancreas (including both PDAC and obstructive pancreatitis lesions) and found that [^{68} Ga]Ga-FAPI-04 and [^{18}F]F-FDG uptake in the whole pancreas can be combined to further stratify postoperative patients' prognoses. The combination of [^{68} Ga]Ga-FAPI-04 and [^{18}F]F-FDG PET/CT imaging can provide clinicians with more comprehensive information for devising the optimal treatment plan. For instance, when patients exhibit lower uptake in both [^{68} Ga]Ga-FAPI-04 and [^{18}F]F-FDG, their postoperative prognosis is better, and more aggressive treatment strategies and closer follow-ups may be needed. Conversely, for PDAC patients with higher uptake in both [^{68} Ga]Ga-FAPI-04 and [^{18}F]F-FDG, their prognosis is the worst, and more conservative treatment strategies can be considered. Besides, we appreciated that patients with pancreatic head cancer and with preoperative obstructive pancreatitis may be a candidate for intensive treatment, such as neoadjuvant treatment [15]. Fibrous stroma and excessive extracellular matrix were also associated with shorter survival of patients with adenocarcinoma [19, 20]. This prognostic variability among individuals with PDAC likely reflects the heterogeneity of tumor metabolism and tumor microenvironment activity [21] since tumor progression, including metastasis, is associated with cellular components in the malignant niche, which dramatically modifies metabolism to accommodate a changing microenvironment [22, 23].

This study had some limitations. First, this was a single-center study with a modest sample size. Therefore, additional studies involving larger patient groups are required to verify these findings. Second, the prognostic assessment of nonsurgical patients was clinically significant; however, fewer nonsurgical patients were recruited in this study to allow for statistical analyses. Third, distant metastatic lesions were not diagnosed pathologically but by follow-up imaging, which may cause a bias in the results due to chemotherapy. Therefore, assessments of pathological and molecular responses using [^{68} Ga]Ga-FAPI-04 PET/CT in patients with PDAC after neoadjuvant chemotherapy are warranted.

Conclusion

[^{68} Ga]Ga-FAPI-04 PET/CT performed better than [^{18}F]F-FDG PET/CT for disease staging, with increased sensitivity and accuracy in patients with PDAC without radiographic metastasis. Additionally, the aggressive pathological characteristics of PDAC significantly correlated with [^{68} Ga]Ga-FAPI-04 rather than [^{18}F]F-FDG. Finally, [^{68} Ga]Ga-FAPI-04 uptake is a non-invasive stromal signature associated with patient survival, and simultaneous [^{68} Ga]Ga-FAPI-04 and [^{18}F]F-FDG uptake examinations improve the accuracy of PDAC diagnoses.

Supplementary information The online version contains supplementary material available at https://doi.org/10.1007/s00259-023-06297-y.

Author contribution All author were involved in the study conception and design. Jie Ding, Zhixin Hao, Hua Huang, Qiaofei Liu, Wenjing Liu, and Chao Ren were involved in acquisition of data. Jie Ding and Jiangdong Qiu were involved in analysis and interpretation of the data. Jie Ding, Xiang Li, and Jiangdong Qiu were involved in drafting of the manuscript. All authors were involved with critical revisions of the manuscript.

Funding This work was sponsored in part by the National Natural Science Foundation of China (Grant No. 82071967), the National Key Research and Development Program of China (Grant No. 2020YFC2002702), CAMS Initiative for Innovative Medicine (No. CAMS-2018-I2M-3–001), CAMS initiative for innovative medicine (2016ZX310174-4), Tsinghua University-Peking Union Medical College Hospital Initiative Scientific Research Program (Grant No. 52300300519), and Capital's Funds for Health Improvement and Research (CFH-2018–2-4014).

Data availability The datasets generated or analyzed during this study are available from the corresponding author on reasonable request.

Declarations

Ethics approval All procedures performed in studies involving human participants were in accordance with the Institutional Ethics Committee of the Peking Union Medical College Hospital (Beijing, China, IRB protocol #ZS1810).

Consent to participate Informed consent was obtained from all individual participants included in the study for publication.

Consent for publication The authors affirm that human research participants provided informed consent for publication of the images in this article.

Conflicts of interest The authors declare no competing interests.

References

1. Mizrahi JD, Surana R, Valle JW, Shroff RT. Pancreatic cancer. Lancet. 2020;395(10242):2008–20. https://doi.org/10.1016/S0140-6736(20)30974-0.
2. Miyazaki M, Yoshitomi H, Shimizu H, Ohtsuka M, Yoshidome H, et al. Repeat pancreatectomy for pancreatic ductal cancer recurrence in the remnant pancreas after initial pancreatectomy: is it worthwhile? Surgery. 2014;155(1):58–66. https://doi.org/10.1016/j.surg.2013.06.050.
3. Scheufele F, Hartmann D, Friess H. Treatment of pancreatic cancer-neoadjuvant treatment in borderline resectable/locally advanced pancreatic cancer. Transl Gastroenterol Hepatol. 2019;4:32. https://doi.org/10.21037/tgh.2019.04.09.
4. Rijkers AP, Valkema R, Duivenvoorden HJ, van Eijck CH. Usefulness of F-18-fluorodeoxyglucose positron emission tomography to confirm suspected pancreatic cancer: a meta-analysis. Eur J Surg Oncol. 2014;40(7):794–804. https://doi.org/10.1016/j.ejso.2014.03.016.

5. Erkan M, Hausmann S, Michalski CW, Fingerle AA, Dobritz M, et al. The role of stroma in pancreatic cancer: diagnostic and therapeutic implications. Nat Rev Gastroenterol Hepatol. 2012;9(8):454–67. https://doi.org/10.1038/nrgastro.2012.115.
6. Niedermeyer J, Kriz M, Hilberg F, Garin-Chesa P, Bamberger U, et al. Targeted disruption of mouse fibroblast activation protein. Mol Cell Biol. 2000;20(3):1089–94. https://doi.org/10.1128/MCB.20.3.1089-1094.2000.
7. Madsen CD. Pancreatic cancer is suppressed by fibroblast-derived collagen I. Cancer Cell. 2021;39(4):451–3. https://doi.org/10.1016/j.ccell.2021.02.017.
8. Röhrich M, Naumann P, Giesel FL, Choyke PL, Staudinger F, et al. Impact of (68)Ga-FAPI PET/CT imaging on the therapeutic management of primary and recurrent pancreatic ductal adenocarcinomas. J Nucl Med. 2021;62(6):779–86. https://doi.org/10.2967/jnumed.120.253062.
9. Zhang Z, Jia G, Pan G, Cao K, Yang Q, et al. Comparison of the diagnostic efficacy of (68) Ga-FAPI-04 PET/MR and (18)F-FDG PET/CT in patients with pancreatic cancer. Eur J Nucl Med Mol Imag. 2022;49(8):2877–88. https://doi.org/10.1007/s00259-022-05729-5.
10. Pang Y, Zhao L, Shang Q, Meng T, Zhao L, et al. Positron emission tomography and computed tomography with [(68)Ga]Ga-fibroblast activation protein inhibitors improves tumor detection and staging in patients with pancreatic cancer. Eur J Nucl Med Mol Imag. 2022;49(4):1322–37. https://doi.org/10.1007/s00259-021-05576-w.
11. Deng M, Chen Y, Cai L. Comparison of 68Ga-FAPI and 18[F] F-FDG PET/CT in the imaging of pancreatic cancer with liver metastases. Clin Nucl Med. 2021;46(7):589–91. https://doi.org/10.1097/RLU.0000000000003561.
12. Nakata B, Amano R, Kimura K, Hirakawa K. Comparison of prognosis between patients of pancreatic head cancer with and without obstructive jaundice at diagnosis. Int J Surg. 2013;11(4):344–9. https://doi.org/10.1016/j.ijsu.2013.02.023.
13. Ding J, Qiu J, Hao Z, Huang H, Liu Q, et al. Prognostic value of preoperative [68 Ga]Ga-FAPI-04 PET/CT in patients with resectable pancreatic ductal adenocarcinoma in correlation with immunohistological characteristics. Eur J Nucl Med Mol Imaging. 2023. https://doi.org/10.1007/s00259-022-06100-4.
14. Tempero MA. NCCN Guidelines Updates: Pancreatic Cancer. J Natl Compr Canc Netw. 2019;17(5.5):603–5. https://doi.org/10.6004/jnccn.2019.5007.
15. Nagtegaal ID, Odze RD, Klimstra D, Paradis V, Rugge M, et al. The 2019 WHO classification of tumours of the digestive system. Histopathology. 2020;76(2):182–8. https://doi.org/10.1111/his.13975.
16. Higashi T, Saga T, Nakamoto Y, Ishimori T, Fujimoto K, et al. Diagnosis of pancreatic cancer using fluorine-18 fluorodeoxyglucose positron emission tomography (FDG PET) –usefulness and limitations in "clinical reality." Ann Nucl Med. 2003;17(4):261–79. https://doi.org/10.1007/BF02988521.
17. Liu Y, Watabe T, Kaneda-Nakashima K, Shirakami Y, Naka S, et al. Fibroblast activation protein targeted therapy using [177Lu]FAPI-46 compared with [225Ac]FAPI-46 in a pancreatic cancer model. Eur J Nucl Med Mol Imaging. 2022;49(3):871–80. https://doi.org/10.1007/s00259-021-05554-2.
18. Xing J, Yang B, Hou X, Jia N, Gong X, et al. Prognostic factors and effect of adjuvant chemoradiation following chemotherapy in resected pancreatic cancer patients with lymph node metastasis or R1 resection. Front Oncol. 2021;11:660215. https://doi.org/10.3389/fonc.2021.660215.
19. Cohen SJ, Alpaugh RK, Palazzo I, Meropol NJ, Rogatko A, Xu Z, et al. Fibroblast activation protein and its relationship to clinical outcome in pancreatic adenocarcinoma. Pancreas. 2008;37(2):154–8. https://doi.org/10.1097/MPA.0b013e31816618ce.
20. Shi M, Yu DH, Chen Y, Zhao CY, Zhang J, Liu QH, et al. Expression of fibroblast activation protein in human pancreatic adenocarcinoma and its clinicopathological significance. World J Gastroenterol. 2012;18(8):840–6. https://doi.org/10.3748/wjg.v18.i8.840.
21. 21.Menezes S, Okail MH, Jalil SMA, Kocher HM, Cameron AJM. Cancer-associated fibroblasts in pancreatic cancer: new subtypes, new markers, new targets. 2022;257(4):526-544. https://doi.org/10.1002/path.5926.
22. Kalluri R. The biology and function of fibroblasts in cancer. Nat Rev Cancer. 2016;16(9):582–98. https://doi.org/10.1038/nrc.2016.73.
23. Xia L, Oyang L, Lin J, Tan S, Han Y, et al. The cancer metabolic reprogramming and immune response. Mol Cancer. 2021;20(1):28. https://doi.org/10.1186/s12943-021-01316-8.

Authors and Affiliations

Jie Ding[1] · Jiangdong Qiu[2] · Zhixin Hao[1] · Hua Huang[2] · Qiaofei Liu[2] · Wenjing Liu[2] · Chao Ren[1] · Marcus Hacker[3] · Taiping Zhang[2] · Wenming Wu[2] · Xiang Li[3] · Li Huo[1]

[1] Department of Nuclear Medicine, Beijing Key Laboratory of Molecular Targeted Diagnosis and Therapy in Nuclear Medicine and State Key Laboratory of Complex Severe and Rare Diseases, Peking Union Medical College (PUMC) Hospital, Chinese Academy of Medical Science and PUMC, No. 1 Shuaifuyuan, Wangfujing Street, Dongcheng District, Beijing 100730, China

[2] Department of General Surgery, PUMC Hospital, Chinese Academy of Medical Sciences and PUMC, No. 1 Shuaifuyuan, Wangfujing Street, Dongcheng District, Beijing 100730, China

[3] Division of Nuclear Medicine, Department of Biomedical Imaging and Image-Guided Therapy, Medical University of Vienna, Vienna, Austria